Journal of Computational Applied Mechanics 2025, 56(3): 627-640

DOI: 10.22059/jcamech.2025.396203.1494

RESEARCH PAPER

A novel frequency formula and its application for a bead sliding on a wire in fractal space

Guang-Qing Feng [a, *], Abdulrahman Ali Alsolami [b]

[a] *School of Mathematics and Information Science, Henan Polytechnic University, Jiaozuo, 454003, China*

[b] *Department of Mathematics, Faculty of Science, King Abdulaziz University, Jeddah, 21589, Saudi Arabia*

Abstract

The present study investigates the frequency-amplitude relationship of a nonlinear oscillator in fractal space, focusing on the dynamics of a bead sliding along a rotating wire with inhomogeneous angular velocity. Utilizing the two-scale fractal theory, the original fractal differential equation is transformed into an equivalent linear damped system in continuous space, thereby enabling the derivation of an exact analytical solution that does not rely on perturbation methods. A novel frequency formula is proposed that integrates fractal parameters and system constants. The establishment of these expressions is achieved through the application of energy conservation principles and Taylor series approximations, thereby providing explicit expressions for the fractal parameters. Numerical simulations were conducted to verify the analytical results and to demonstrate the influence of the parameters on damping behavior and oscillation profiles. The proposed framework is a versatile analytical tool for the study of fractal-mediated dynamics in mechanical systems, with potential applications in resonant engineering and multiscale materials design.

Keywords: Fractal space mechanics; nonlinear oscillator; two-scale fractal theory; frequency-amplitude relationship; numerical simulation; Multiscale system response; Bead-on-wire dynamics; Nonlinear frequency analysis

1. Introduction

Differential equations represent a foundational component of scientific and engineering disciplines, providing a crucial framework for the modeling of a wide array of physical phenomena. Of particular importance are nonlinear oscillator models in mechanical systems, quantum physics, and astrophysics, where second-order nonlinear differential equations are central to dynamic simulations and control applications. Despite their ubiquity, exact analytical solutions for such equations remain elusive in most cases, requiring the development of sophisticated approximation techniques or numerical methods. Differential equations represent a foundational component of scientific and engineering disciplines, providing a crucial framework for the modeling of a wide array of physical phenomena. Of particular importance are nonlinear oscillator models in mechanical systems, quantum physics, and

* Corresponding author. Tel.: 13723198094. *E-mail address:* fgqing@hpu.edu.cn

astrophysics, where second-order nonlinear differential equations are central to dynamic simulations and control applications. Despite their ubiquity, exact analytical solutions for such equations remain elusive in most cases, requiring the development of sophisticated approximation techniques or numerical methods. Recent advancements in nonlinear sciences have led to an escalation in research endeavors focused on fractal-influenced oscillatory systems, with a pivotal emphasis on deriving exact solutions for fractal nonlinear oscillators without resorting to perturbation methods. This challenge is further compounded by the inherent complexity of obtaining analytical approximations compared to numerical counterparts. Recent advancements in nonlinear sciences have prompted a surge in research endeavors centered on fractal-influenced oscillatory systems. A pivotal emphasis has emerged on deriving exact solutions for fractal nonlinear oscillators, eschewing the use of perturbation methods. This challenge is further compounded by the inherent complexity of obtaining analytical approximations compared to numerical counterparts.

The interplay between nonlinear dynamics and fractal geometry has yielded profound insights into complex systems characterized by self-similarity and scale invariance. Since its inception, fractal theory has transcended mathematical abstraction to address real-world phenomena in fluid mechanics, materials science, and energy transport. Notable applications include the modeling of thermal conductivity in branched networks [1, 2], the characterization of the properties of composite materials [3], and the description of the rheological behavior of non-Newtonian fluids [4]. The advent of two-scale fractal theory has further expanded this paradigm, facilitating multiscale analysis of both continuous and discrete systems [5-7]. He et al. advanced this field by proposing a two-scale fractal oscillation model and demonstrated its effectiveness in addressing complex fractional systems [8].

Fractal nonlinear vibrations are notable for their mathematical elegance and capacity to serve as a bridge between theoretical constructs and practical engineering challenges. These systems inherently capture the nonlinear essence of real-world phenomena. In this regard, scholars have employed fractal-based formulations to analyze complex dynamic behaviors in diverse systems. For instance, Elias-Zuniga et al. [9] investigated the dynamic response of non-Gaussian polymer chains using fractal equations, thereby underscoring the adaptability of fractal frameworks in modeling intricate interactions. In a related context, Song [10] developed a thermodynamic framework for packed dynamical systems by integrating fractal principles. Furthermore, Bayat et al. [11] systematically reviewed advancements in asymptotic methodologies, emphasizing their utility in addressing nonlinear vibration problems, which has significantly enriched the theoretical exploration of fractal-related mechanisms. The critical relationship between frequency and amplitude in such systems has driven methodological innovations, including the homotopy perturbation method [12-15], the variational iteration method [16, 17], and the harmonic balance method [18, 19]. Conventional techniques for analyzing nonlinear oscillators have proven effective in many cases. Notably, the advent of fractal calculus and conservation principles has had a profound influence on contemporary methodologies, facilitating solutions to nanoparticle vibrations [20, 21] and nonlinear MEMS dynamics [22-25]. Despite these advancements, existing frequency-amplitude formulations frequently lack iterative refinement capabilities. This limitation is addressed by El-Dib's progressive frequency formula [26, 27], which facilitates successive approximations for nonlinear vibrations.

This study presents a systematic investigation of fractal nonlinear oscillators through frequency-amplitude analysis, building on the basic framework. The approach adopted in this study eliminates the necessity of perturbation techniques by transforming the fractal oscillator into an equivalent linear damped system. This transformation facilitates the derivation of exact analytical solutions. The fractal parameters are estimated with a high degree of accuracy, and explicit amplitude-frequency relationships are established through the application of energy conservation principles. The proposed methodology circumvents the limitations of traditional approaches and provides a versatile tool for analyzing fractal-mediated dynamics in various engineering applications. By elucidating these relationships, this work advances both the theoretical understanding and practical manipulation of complex vibrational systems in fractal spaces.

2. Frequency-amplitude analysis of a nonlinear oscillator

Consider a general nonlinear oscillator as follows

$$\frac{d^2z}{d\tau^2} + h(z) = 0, z(0) = a, z'(0) = b \tag{1}$$

where $h(z)$ is defined as the nonlinear restoring force, and z as the displacement. a and b are constants.

The linearized form of Eq. (1) is a second-order linear differential equation as

$$\frac{d^2z}{d\tau^2} + \omega^2 z = 0 \tag{2}$$

The corresponding frequency formulation is given by [28-32]

$$\omega^2 = \lim_{z \to \frac{1}{2}A} \frac{dh(z)}{dz} \tag{3}$$

Its solution that satisfies the initial conditions is

$$z = a\cos\omega\tau + \frac{b}{\omega}\sin\omega\tau = A\cos(\omega\tau + \phi) \tag{4}$$

Obviously, the amplitude A and the angle ϕ in the above formula have the following form

$$A = \sqrt{a^2 + \frac{b^2}{\omega^2}} \tag{5}$$

$$\phi = \arctan(-\frac{b}{a\omega}) \tag{6}$$

While formula (3) has been extensively validated for cubic polynomials of the function $h(z)$, its applicability is inherently constrained by the exclusion of velocity terms z' or z'', and their nonlinear combinations. To address these limitations, He [33] introduced an enhanced formulation that enables systematic investigation of frequency-amplitude relationships in nonlinear oscillators characterized by irrational nonlinearities.

Consider a more general form of a nonlinear oscillator described by the equation

$$\frac{d^2z}{d\tau^2} + H(z, \frac{dz}{d\tau}, \frac{d^2z}{d\tau^2}) = 0, z(0) = a, \frac{d}{d\tau}z(0) = b \tag{7}$$

where H represents a function of z and its derivatives. The corresponding frequency formulation is given by

$$\omega^2 = \lim_{z \to \frac{1}{2}A, \frac{dz}{d\tau} \to -\frac{\sqrt{3}}{2}\omega A, \frac{d^2z}{d\tau^2} \to -\frac{1}{2}\omega^2 A} \frac{dH}{dz} \tag{8}$$

This method provides new insights into the complex dynamics of nonlinear oscillators and offers practical implications for fields such as spanning physics, mechanical engineering, and nonlinear applied mathematics. The developed framework collectively enables a paradigm shift from idealized oscillator models to functionally adaptive systems with embedded intelligence capabilities.

3. Frequency-amplitude analysis for fractal nonlinear oscillation

The fractal theory, with its inherent capacity to formulate governing equations within geometrically complex fractal spaces, has emerged as a pivotal research frontier across applied mathematics and mechanical engineering disciplines. This paradigm provides rigorous mathematical frameworks for analyzing multiscale phenomena, from porous media transport to nonlinear vibration analysis in heterogeneous materials.

The two-scale fractal derivative [34] is defined as follows

$$\frac{dz}{dt^{\varphi}}(t_0) = \Gamma(1+\varphi) \lim_{t - t_0 \to \Delta t, \Delta t \neq 0} \frac{z(t) - z(t_0)}{(t - t_0)^{\varphi}} \tag{9}$$

where $z(t)$ is a function, Γ denotes the Gamma function, and Δt signifies the lowest hierarchical time level. This fractal derivative is conceptualized as the natural development of the Leibniz derivative, specifically for discontinuous fractal media. φ represents the fractal dimension in the time-direction. It quantifies the degree of temporal non-uniformity or "fractalness" of the underlying space.

Two-scale fractal theory provides an indispensable analytical framework for reconciling macroscopic continuity with microscale discontinuity in dynamical systems. This dual-perspective approach enables rigorous quantification of scale-dependent transitions between smooth and fragmented spatial-temporal patterns, offering unprecedented precision in multiscale system characterization, ranging from porous media dynamics to quantum-classical interface phenomena.

The conventional continuous space model of a nonlinear oscillator posits the assumption that the medium is uniform and the dimension is an integer. However, for certain dynamic processes, the interpretation of continuous space models can present significant challenges. This necessity has prompted the exploration of nonlinear oscillators within the framework of fractal space. The fractal space exhibits characteristics such as fractal dimension, self-similarity, and multi-scale nesting, which are not present in continuous space. To establish an oscillator model in fractal space, it is necessary to assume $\tau = t^{\varphi}(0 < \varphi < 1)$, we have

$$\frac{d}{d\tau} \to \frac{d}{dt^{\varphi}}, \quad \frac{d^2}{d\tau^2} \to \frac{d^2}{dt^{2\varphi}}$$

The following is the transformation of the governing equation with fractional temporal variation from the original Eq. (7)

$$\frac{d^2 z}{dt^{2\varphi}} + H\left(z, \frac{dz}{dt^{\varphi}}, \frac{d^2 z}{dt^{2\varphi}}\right) = 0, \; z(0) = a, \; \frac{dz(0)}{dt^{\varphi}} = b \tag{10}$$

It is noteworthy that the two-scale fractal derivative agrees with the traditional differential derivative when the fractal dimension, designated by the symbol φ, is a positive integer. It exhibits the following properties:

$$\frac{dz}{dt^{1}} = \Gamma(1+1) \lim_{t - t_0 \to \Delta t, \Delta t \neq 0} \frac{z(t) - z(t_0)}{(t - t_0)^1} = z'.$$

A critical inquiry emerges concerning the dynamics in fractal space. Considering the properties delineated below, it can be inferred that

$$\frac{dz}{dt^{\varphi}} = p(\varphi) z + q(\varphi) z' \tag{11}$$

The analysis is set up to tackle the unknowns $p(0) \to 1$, $q(0) \to 0$, $p(1) \to 0$, and $q(1) \to 1$. Based on El-Dib's studies [35, 36], the following proposal is put forward:

$$\frac{dz}{dt^{\varphi}} = S^{\varphi} \cos\frac{\pi\varphi}{2} z + S^{\varphi - 1} \sin\frac{\pi\varphi}{2} z' \tag{12}$$

where S is a real constant indicating a fractalness parameter (non-homogeneity parameter) of the medium, depending on the fractal dimension φ to be determined later. The parameter S emerges as a crucial link between the fractal description and the equivalent continuous dynamics.

Consequently, Eq. (10) can be verified that

$$z'' + H^{*}(z, z', z'') = 0 \tag{13}$$

This is the alternative form of the fractal Eq. (10) in continuous space. The alternative initial conditions in the continuous space are performed in the form

$$z(0) = a, z'(0) = bS^{1-\varphi} scs \frac{\pi\varphi}{2} - aS \cot \frac{\pi\varphi}{2} \tag{14}$$

The transformation technique presented here fundamentally converts the fractal temporal derivative into an equivalent system in continuous space featuring both an effective conservative force term and an effective linear damping term. This exemplifies a fundamental strength of the approach, as it inherently accommodates dissipative behavior arising from the fractal nature of time or space.

In the context of systems that possess intrinsic or native damping terms, the applicability of the aforementioned procedure necessitates meticulous examination. The transformation defined by Eq. (12) is applied to the entire governing equation (Eq. (10)). If Eq. (10) contains an explicit velocity-dependent damping term, the transformation will map this term into the continuous space equation (Eq. (13)) as well. The resulting transformed equation would then combine the effective damping from the fractal transformation and the transformed native damping term. Subsequent frequency-amplitude analysis (Eq. (15)) and solution derivation would need to account for this combined dissipative effect. While the fundamental transformation principle remains valid, the specific forms of P, Q, and the frequency expression may become more complex. The subsequent expansion of the method to encompass native damping necessitates dedicated investigation in future studies. This investigation will build upon the foundational work presented here, focusing on the undamped case and the intrinsic dissipation modeled by fractal time.

The corresponding frequency formulation is given by

$$\omega^2 = \lim_{z \to \frac{1}{2}A, z' \to -\frac{\sqrt{3}}{2}\omega A, z'' \to -\frac{1}{2}\omega^2 A} \frac{dH^*(z, z', z'')}{dz} \tag{15}$$

where

$$A = \sqrt{(z(0))^2 + \frac{(z'(0))^2}{\omega^2}} \tag{16}$$

The frequency-amplitude relationship has been a central subject of extensive investigation in the field of nonlinear dynamics. Throughout its theoretical development, this relationship has undergone numerous refinements. This formula has evolved into a powerful analytical tool for characterizing nonlinear oscillatory systems. Eq. (15) proposes an innovative frequency-amplitude formulation that demonstrates particular effectiveness in the rapid exploration of fractional-order system properties. Building upon this foundational framework, we subsequently apply the proposed formulation to obtain a precise analytical solution for a fractal nonlinear system. We specifically examine the dynamics of a bead sliding along a wire shaped like a vertical parabola, as illustrated in Fig. 1.

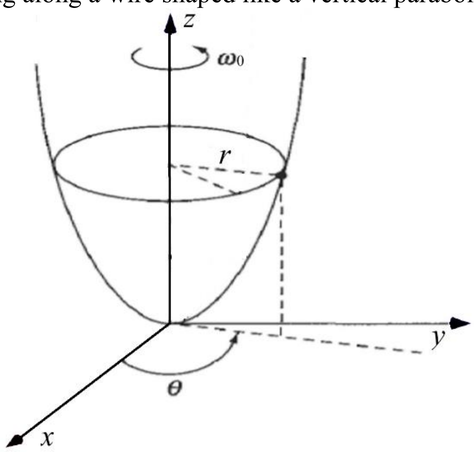

Fig 1: sketch for a bead sliding on a wire

The trajectory of the bead is circular, with a radius designated as r, and the wire undergoes rotation with an angular velocity, denoted as $\omega(t)$, around its vertical symmetry axis. Here, $\omega(t)$ is equivalent to a constant angular velocity, designated as ω_0. The coordinates that delineate this scenario are cylindrical in nature (r, θ, z). The explicit temporal dependence on angular rotation is represented by $\theta = \omega_0 \tau$. The constant c, representing the rate of rotation, enables the parabola's equation to be expressed as $z = cr^2$. The equation of motion in the smooth wire conserves the independent variable τ in continuous space, while it is necessary to investigate the impact of non-homogeneous spatial variation on the sliding bead motion. In numerous practical engineering scenarios, the assumption of constant angular velocity ($\omega(t)= \omega_0$) may not be valid. Non-homogeneous angular velocity $\omega(t)$ can emerge from a variety of sources, including variable-speed machinery, micro-electro-mechanical systems (MEMS), granular flow and particle separation, and geophysical analogs. Components of rotating machinery, including turbines and centrifuges, are susceptible to fluctuations in driving torque or load, which can result in variations in operational speed. In the context of MEMS gyroscopes and resonators, the presence of rotating elements renders them susceptible to external vibrations or control signals that induce speed modulations. In the context of scientific inquiry, the phenomenon of particles sliding on rotating surfaces, as observed in cyclones or spiral separators, is of particular interest. The dynamics of flow and the interactions between surfaces are known to induce non-uniform rotational motion, thereby creating a complex and dynamic environment for study. The model simplified aspects of motion along fault lines or geological structures exhibiting fractal roughness under non-uniform tectonic stresses.

It is imperative to comprehend the dynamics of a bead under such non-uniform rotation $\omega(t)$ within a fractal space framework, as elucidated in this study, to facilitate the analysis and design of systems where friction, wear, particle transport, or resonant behavior occurs under complex rotational conditions and multiscale geometries.

Assuming the angular rotation is expressed in fractional form $\omega_0 \tau = t^{\varphi}, 0 < \varphi < 1$. The governing equation of motion for a smooth wire with fractional temporal variation is [37, 38]

$$\frac{d^2 r}{dt^{2\varphi}} + \frac{2gc - \omega_0^2}{\omega_0^2(1 + 4c^2 r^2)} r + \frac{4c^2 r}{1 + 4c^2 r^2} \left(\frac{dr}{dt^{\varphi}}\right)^2 = 0, r(0) = a, \frac{dr(0)}{dt^{\varphi}} = 0 \quad (17)$$

Eq. (17) involves several key parameters. The parameters a, ω_0, g, and c are initial conditions or fundamental physical constants that define the specific mechanical system under study. The parameter a denotes the initial radial displacement of the bead, measured in the Imperial System of Units as feet (*ft*). It represents the amplitude of the initial perturbation. The base angular velocity, designated as ω_0, is measured in radians per second (*rad*/*s*), and it characterizes the nominal rotational speed of the wire. In the non-homogeneous case, the symbol often represents a characteristic scale or average value. g represents the acceleration due to gravity on Earth (Imperial units: ft/s^2, as used in simulations). This quantity represents the constant gravitational force acting on the bead. The parameter c is the parabolic constant, measured as ft^{-1}. The parabolic wire's shape is defined by the equation $z = cr^2$, and its steepness is determined by the equation's parameters.

In the domain of physics, the objective is to approximate a suitable solution to Eq. (17) within the context of fractal space. A pragmatic approach entails the conversion of this equation into a form that employs the conventional derivative in continuous space. This necessitates converting the assignments of the traditional derivative, as delineated in Eq. (12), into the format of the equation of motion (17) coupled with the initial conditions, resulting in a formulation that can be expressed as

$$r'' + H^*(r, r', r'') = 0, r(0) = a, r'(0) = -aP \quad (18)$$

where H^* has the form

$$H^*(r, r', r'') = (P^2 + \frac{2gc - \omega_0^2}{\omega_0^2 Q^2})r + 8P^2 c^2 r^3 + 2P r' + 16Pc^2 r^2 r' + 4c^2 r r'^2 + 4c^2 r^2 r'' \quad (19)$$

The notation P and Q are given by

$$P = S \cot \frac{\pi\varphi}{2}, Q = S^{\varphi-1} \sin \frac{\pi\varphi}{2} \quad (20)$$

The frequency form (15) can be used to obtain

$$\omega^2 = \frac{dH^*(r, r', r'')}{dr} = P^2 + \frac{2gc - \omega_0^2}{\omega_0^2 Q^2} + 24P^2c^2r^2 + 4c^2(8Pr + r')r' + 16c^2 r r'' \\ +2P(1 + 8c^2r^2)\frac{r''}{r'} + 4c^2r^2\frac{r'''}{r'} \tag{21}$$

Substituting these expressions $A = \sqrt{a^2 + \frac{(aP)^2}{\omega^2}}$, $r = \frac{1}{2}A, r' = -\frac{\sqrt{3}}{2}\omega A, r'' = -\frac{1}{2}\omega^2 A, r''' = \frac{\sqrt{3}}{2}\omega^3 A$ into Eq. (21) yields

$$(1 + 2c^2a^2)\omega^4 + (\frac{20}{\sqrt{3}}c^2a^2 - \frac{2}{\sqrt{3}})P\omega^3 - [(1 + 4c^2a^2) + \frac{2gc - \omega_0^2}{\omega_0^2 P^2 Q^2}]P^2\omega^2 \\ + \frac{20}{\sqrt{3}}c^2a^2P^3\omega - 6c^2a^2P^4 = 0 \tag{22}$$

The determination of the parameter S is necessary to ascertain the expressions of P and Q. Given that Eq. (18) is a counterpart of Eq. (17), a comparison of the linear frequency of this transformed equation with the linear frequency of the original nonlinear oscillator yields a significant relation. This relation intricately connects the constant c and the angular frequency ω_0 in terms of the fractal parameter φ, illustrating a critical linkage between these fundamental parameters within the context of the fractal space. To select the coefficient of the first term of r in Eq. (17), Taylor's representation of $1/(1+4c^2r^2)$ is used to obtain the coefficient of the first term as $(2gc-\omega_0^2)/\omega_0^2$. The coefficient of the first term of r in Eq. (18) is $P^2+(2gc-\omega_0^2)/(\omega_0^2Q^2)$. By equating these coefficients, we derive

$$\frac{P^2Q^2}{Q^2 - 1} = \frac{2gc - \omega_0^2}{\omega_0^2} \tag{23}$$

Combining the relationship between P and Q in Eq. (23), Eq. (22) becomes

$$(1 + 2c^2a^2)\omega^4 + (\frac{20}{\sqrt{3}}c^2a^2 - \frac{2}{\sqrt{3}})P\omega^3 - (4c^2a^2P^2 + \frac{2gc - \omega_0^2}{\omega_0^2})\omega^2 + \frac{20}{\sqrt{3}}c^2a^2P^3\omega - 6c^2a^2P^4 = 0 \tag{24}$$

It can be reduced

$$2c^2a^2(\omega^2 + P^2)(\omega^2 + \frac{10}{\sqrt{3}}P\omega - 3P^2) + \omega^2(\omega^2 - \frac{2}{\sqrt{3}}P\omega - \frac{2gc - \omega_0^2}{\omega_0^2}) = 0 \tag{25}$$

To make Eq. (25) physically meaningful, the inequality $(\omega^2 + \frac{10}{\sqrt{3}}P\omega - 3P^2)(\omega^2 - \frac{2}{\sqrt{3}}P\omega - \frac{2gc - \omega_0^2}{\omega_0^2}) < 0$ must be satisfied. Solving this inequality yields the permissible range of ω as:

$$\frac{\sqrt{34}-5}{\sqrt{3}}P < \omega < \frac{1}{\sqrt{3}}P + \sqrt{\frac{1}{3}P^2 + \frac{2gc-\omega_0^2}{\omega_0^2}} \tag{26}$$

Substitution of Eq. (20) into (23) yields

$$S^{2\varphi} - \frac{2gc-\omega_0^2}{\omega_0^2}\tan^2\left(\frac{\pi\varphi}{2}\right)S^{2\varphi-2} + \frac{2gc-\omega_0^2}{\omega_0^2}\sec^2\left(\frac{\pi\varphi}{2}\right) = 0 \tag{27}$$

The parameter S is represented in a complicated transcendental manner, contingent on the parameter φ and the coefficient of the original equation. Once the value of the parameter of interest is ascertained, the value of the parameter S will be established. As illustrated in Fig. 2, the relationship between φ and S is depicted for various values of $(2gc-\omega_0^2)/\omega_0^2$, ranging from 0.01 (weak coupling) to 100 (strong coupling). Key observations are as follows:

Weak Coupling ($(2gc\text{-}\omega_0^2)/\omega_0^2 \ll 1$): For $(2gc\text{-}\omega_0^2)/\omega_0^2=0.01$, S remains nearly constant over a wide range of φ, as the small coefficient suppresses the nonlinear terms in Eq. (27). A slight rise in S at larger φ is attributed to the residual influence of the sec^2 term.

Intermediate Coupling ($(2gc\text{-}\omega_0^2)/\omega_0^2=1$): At $(2gc\text{-}\omega_0^2)/\omega_0^2=1$, the solution transitions smoothly, with S increasing monotonically as φ increases. The interplay between tan^2 term and sec^2 term introduces a gradual curvature, reflecting the competition between exponential and trigonometric dependencies.

High Coupling Regime ($(2gc\text{-}\omega_0^2)/\omega_0^2 \gg 1$): For $(2gc\text{-}\omega_0^2)/\omega_0^2=100$, S exhibits a sharp increase as φ approaches 1. This behavior arises from the dominance of the $\tan^2$ term in Eq. (27), which diverges at $\varphi\to1$, necessitating $S\to1$ to balance the equation.

Notably, all curves converge to $S\to1$ as $\varphi\to1$, consistent with the asymptotic singularity of $\tan^2(\pi\varphi/2)$. These results highlight the sensitivity of S to both φ and the coupling parameter $(2gc\text{-}\omega_0^2)/\omega_0^2$, underscoring the need for precise parameterization in applications such as resonant systems or nonlinear oscillators where such equations commonly arise.

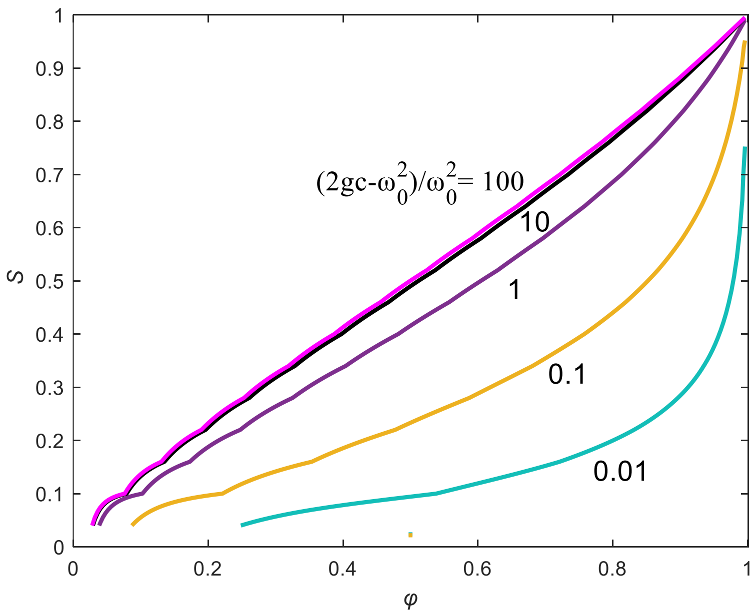

Fig 2: the relationship between φ and S of Eq. (27)

However, it should be noted that the aforementioned formula is incapable of yielding the display solution of *S*. Consequently, the analytical expressions of *P* and *Q* remain elusive. Employing the definition of *P* given in Eq. (20), it yields

$$S^2 = \frac{2gc - \omega_0^2}{\omega_0^2}\tan^2\left(\frac{\pi\varphi}{2}\right)\frac{Q^2 - 1}{Q^2}\,(Q^2 > 1) \tag{28}$$

Eq. (28) is then substituted into the definition of *Q*,

$$\left(\frac{2gc - \omega_0^2}{\omega_0^2}\right)^{\varphi-1}\tan^{2\varphi}\left(\frac{\pi\varphi}{2}\right)\cos^2\left(\frac{\pi\varphi}{2}\right) = Q^2\left(1 - \frac{1}{Q^2}\right)^{1-\varphi} \tag{29}$$

By Taylor series, $\left(1 - \frac{1}{Q^2}\right)^{1-\varphi} = 1 + (\varphi - 1)\frac{1}{Q^2} + \cdots$, it yields

$$Q^2 = \left(\frac{2gc - \omega_0^2}{\omega_0^2}\right)^{\varphi-1}\tan^{2\varphi}\left(\frac{\pi\varphi}{2}\right)\cos^2\left(\frac{\pi\varphi}{2}\right) + 1 - \varphi \tag{30}$$

So, the expression of *P* is

$$P^2 = \frac{2gc - \omega_0^2}{\omega_0^2}\left[1 - \frac{1}{\left(\frac{2gc - \omega_0^2}{\omega_0^2}\right)^{\varphi-1}\tan^{2\varphi}\left(\frac{\pi\varphi}{2}\right)\cos^2\left(\frac{\pi\varphi}{2}\right) + 1 - \varphi}\right] \tag{31}$$

4. Graphical illustration

The ensuing figures offer a visual representation of the precise solution to Eq. (18), which corresponds to Eq. (17) in fractal space. Fig. 3 presents a comparative analysis of results under varying φ values, emphasizing the influence of φ on the system's dynamic behavior. The system parameters are g=32 ft/s^2, ω_0=1.0 rad/s, a=0.2 ft, and c=0.1 ft^{-1}. As the value of φ increases, the analytical solution exhibits enhanced nonlinear effects or damping adjustments, manifested through convergence variations in waveform amplitudes or adaptive changes in oscillation frequencies. The utilization of color or line style to differentiate curves corresponding to different φ values underscores the pivotal role of parametric sensitivity analysis in elucidating the system's dynamical mechanisms.

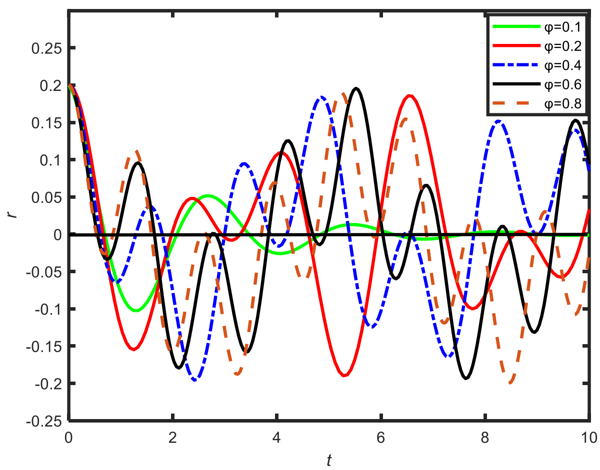

Fig.3: A comparative analysis of Eq. (18) under varying φ values with g=32 ft/s^2, ω_0=1.0 rad/s, a=0.2 ft, and c=0.1 ft^{-1}

The effect of the parameter c on damping and wave profile has been shown in Fig. 4. This graph significantly contributes to the visual interpretation of Eq. (18), and shows that damping behavior is influenced by variations in c. Different c values leads to distinctive damping curve shapes. Fig. 5 shows the periodic solutions for different values of a.

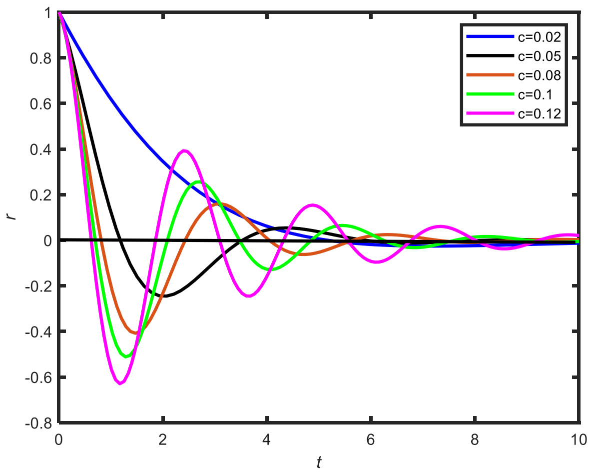

Fig.4: A comparative analysis of Eq. (18) under varying c values with g=32 ft/s^2, ω_0=1.0 rad/s, a=1.0 ft, and φ=0.1

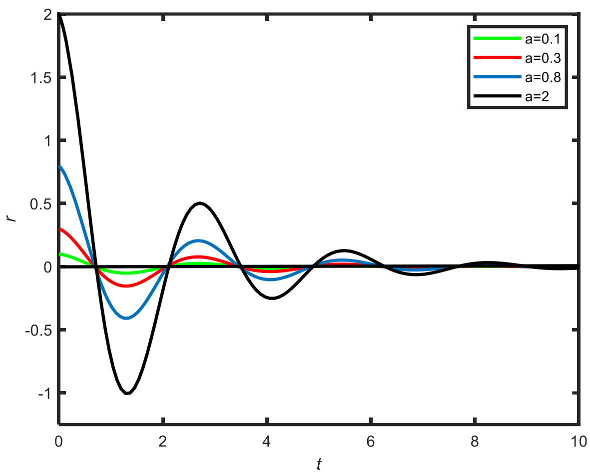

Fig.5: A comparative analysis of Eq. (18) under varying a values with g=32 ft/s^2, ω_0=1.0 rad/s, c=0.1 ft^{-1} and φ=0.1

The linearized version of Eq. (18) is designed to preserve the fundamental dynamical attributes of the original system while simplifying its complexity, as illustrated below:

$$r'' + \omega^2 r = 0, r(0) = a, r'(0) = -aP \tag{32}$$

The primary objective of this paper is to ascertain the conservative frequency ω^2, which is a crucial factor for accurately understanding and representing the dynamic behavior of the system. We have derived expressions for P and Q, as presented in the Eqs. (30) and (31). The precise solution to Eq. (32), which concurrently serves as an approximate solution to Eq. (18), exhibits the following form.

$$r = a\left(\cos \omega t - \frac{P}{\omega}\sin \omega t\right) \tag{33}$$

However, the periodic solution exhibited in Eq. (33) signifies a constant amplitude of motion, while the amplitude of the periodic motion of the system is subject to variation, as demonstrated in Figs. 3 and 4. To ascertain a more precise approximate periodic solution, Eq. (18) is rewritten as

$$r'' + 2(1 + 8c^2r^2)Pr' + H^{**}(r, r', r'') = 0, r(0) = a, r'(0) = -aP \tag{34}$$

where H^{**} has the form

$$H^{**}(r, r', r'') = (P^2 + \frac{2gc - \omega_0^2}{\omega_0^2 Q^2})r + 8P^2c^2r^3 + 4c^2rr'^2 + 4c^2r^2r'' \tag{35}$$

The linearized version of Eq. (34) is designed to preserve the fundamental dynamical attributes of the original system while simplifying its complexity, as illustrated below:

$$r'' + \delta r' + w^2 r = 0 \tag{36}$$

The symbols δ and w^2 are utilized to denote the damping coefficient and the conservative frequency, respectively. The total frequency is denoted by w^2, which has the expression $W^2 = w^2 - \frac{\delta^2}{4}$. They can obtain by Eq. (15),

$$\delta = \frac{d[2(1 + 8c^2r^2)Pr']}{dr'}\Big|_{r=\frac{1}{2}A, r'=-\frac{\sqrt{3}}{2}WA, r''=-\frac{1}{2}W^2A} = 2P(1 - 10c^2a^2 - 10\frac{c^2a^2P^2}{W^2}) \tag{37}$$

$$w^2 = \frac{dH^{**}(r, r', r'')}{dr}\Big|_{r=\frac{1}{2}A, r'=-\frac{\sqrt{3}}{2}WA, r''=-\frac{1}{2}W^2A} = [(1 + 4c^2a^2) + \frac{2gc - \omega_0^2}{\omega_0^2 P^2 Q^2}]P^2 + 6\frac{c^2a^2P^4}{W^2} - 2c^2a^2W^2 \tag{38}$$

Substituting Eqs. (37) and (38) into the expression $W^2 = w^2 - \frac{\delta^2}{4}$ and combining it with Eq. (23) leads to the following simplified equation

$$\begin{aligned} &(1 + 2c^2a^2)W^6 + (1 - 24c^2a^2 + 100c^4a^4 - \frac{2gc - \omega_0^2}{\omega_0^2 P^2})P^2W^4 \\ &+(200c^4a^4 - 26c^2a^2)P^4W^2 + 100c^4a^4P^6 = 0 \end{aligned} \tag{39}$$

The proposed Eq. (36) is characterized by its simplicity, which is expressed in a specific form that reflects the direct nature of the equation. The capacity to derive an accurate solution from such a simplified equation is advantageous because it provides a clear insight into the behavior of the system and helps validate the effectiveness of the linearization and approximation methods used in the analysis. This exact solution form is a pivotal component in comprehending the dynamics and properties of the system delineated in Eq. (36). The solution has the following form

$$r = ae^{-\frac{\delta}{2}t}(\cos Wt + \frac{(\delta - 2P)}{2W}\sin Wt) \tag{40}$$

Fig. 6 compares the numerical solution of Eq. (18) with the analytical solution and shows the agreement. These visualizations are crucial in demonstrating the precision and effectiveness of the analytical solution derived using the frequency method.

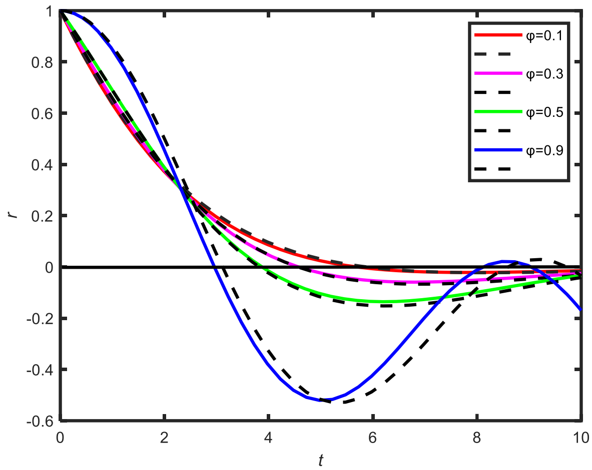

Fig.6: A comparison between the numerical solution for Eq. (18) (solid line) and the exact solution (40) (dashed line) with g=32 ft/s^2, ω_0=2.0 rad/s, a=1 ft, and c=0.08 ft^{-1}

5. Conclusion

This study employs a systematic approach to analyzing fractal nonlinear oscillators through frequency-amplitude relationships. The investigation has yielded significant insights into the intricate dynamics of such systems. A novel frequency formula for fractal systems is derived by transforming the governing equation into a linearized form, circumventing the conventional limitations imposed by perturbation theory. The explicit dependence of fractal parameters (S, P, Q) on φ and coupling strength is rigorously quantified. The numerical results obtained from this study demonstrate that the fractal dimension, denoted by the parameter φ, exerts a substantial influence on oscillation damping and frequency. Furthermore, it is observed that the magnitude of coupling has a direct impact on the sensitivity of the fractal parameter S to parameter φ. The analytical solution (39) exhibits a high degree of congruence with numerical simulations, thereby substantiating the efficacy and precision of the method employed. This framework is adaptable to engineering systems involving fractal geometries, such as porous media transport or MEMS resonators. While the current formulation successfully handles the effective dissipation induced by fractal time, extending the methodology to explicitly incorporate native damping terms into the original fractal governing equation represents a valuable direction for future research. Future endeavors should explore time-dependent fractal dimensions and experimental validation in physical systems such as variable-speed rotating MEMS devices or particle transport systems exhibiting fractal interfaces. Furthermore, extending this approach to higher-dimensional fractal spaces has the potential to further bridge the gap between theoretical models and real-world applications.

Declaration of Competing Interest

The authors declare that - there are no known competing financial interests or personal relationships that could have appeared to influence the work reported in this paper.

Funding

This research did not receive any specific grant from funding agencies in the public, commercial, or not-for-profit sectors.

References

[1] G. Y. Zhang, J. Gao, B. Q. Xiao, L. Chen, J. Y. Cao, G. B. Long, H. R. Hu, Fractal study on the permeability of power-law fluid in a rough and damaged tree-like branching network, *Phys. Fluids,* Vol. 36, 2024.

[2] M. X. Liu, J. Gao, B. Q. Xiao, P. L. Wang, H. Z. Y. Li, S. F. Li, G. B. Long, Y. Xu, Fractal model for effective thermal conductivity of composite materials embedded with a damaged tree-like bifurcation network, *Fractals,* Vol. 32, 2024.

[3] P. Zhang, J. Y. Ding, J. J. Guo, F. Wang, Fractal analysis of cement-based composite microstructure and its application in evaluation of macroscopic performance of cement-based composites: a review, *Fractal Fract,* Vol. 8, 2024.

[4] M. Ungarish, Self-similar flow of Newtonian and power-law viscous gravity currents in a confining gap in rectangular and axisymmetric geometries, *J. Fluid Mech,* Vol. 1007, 2025.

[5] N. Anjum, C. H. He, J. H. He, Two-scale fractal theory for the population dynamics *Fractals,* Vol. 29, 2021.

[6] N. Anjum, Q. T. Ain, X. X. Li, Two-scale mathematical model for tsunami wave, *Gem-Int. J. Geomat,* Vol. 12, pp. 1-12, 2021.

[7] Y. R. Zhang, N. Anjum, D. Tian, A. A. Alsolami, Fast and accurate population forecasting with two-scale fractal population dynamics and its application to population economics, *Fractals,* Vol. 32, 2024.

[8] J. H. He, Y. O. El-Dib, A tutorial introduction to the two-scale fractal calculus and its application to the fractal Zhiber-Shabat oscillator, *Fractals,* Vol. 29, 2021.

[9] A. Elias-Zuniga, O. Martinez-Romero, D. O. Trejo, L. M. Palacios-Pineda, Fractal equation of motion of a non-Gaussian polymer chain: investigating its dynamic fractal response using an ancient Chinese algorithm, *J. Math. Chem,* Vol. 60, pp. 461-473, 2022.

[10] H. Y. Song, A thermodynamic model for a packing dynamical system, *Thermal Science,* Vol. 24, pp. 2331-2335, 2020.

[11] M. Bayat, I. Pakar, M. Bayat, M. Bayat, I. Pakar, M. Bayat, Recent developments of some asymptotic methods and their applications for nonlinear vibration equations in engineering problems: a review, *Lat. Am. J. Solids Struct,* Vol. 9, pp. 145-234, 2012.

[12] B. Moussa, M. Youssouf, N. A. Wassiha, P. Youssouf, Homotopy perturbation method to solve Duffing-Van der Pol equation, *Adv. Differ. Equ. Control Process,* Vol. 31, pp. 299-315, 2024.

[13] G. Q. Feng, Higher-order homotopy perturbation method for the fractal rotational pendulum oscillator, *J. Vib. Eng. Technol,* Vol. 12, pp. 2829-2834, 2024.

[14] J. H. He, C. H. He, A. A. Alsolami, A good initial guess for approximating nonlinear oscillators by the homotopy perturbation method, *Facta Univ. Ser. Mech. Eng,* Vol. 21, No. 1, pp. 21-29, 2023.

[15] N. A. M. Alshomrani, W. G. Alharbi, I. M. A. Alanazi, L. S. M. Alyasi, G. N. M. Alrefaei, S. A. Al'Amri, A. H. Q. Alanzi, Homotopy perturbation method for solving a nonlinear system for an epidemic, *Adv. Differ. Equ. Control Process,* Vol. 31, pp. 347-355, 2024.

[16] N. Anjum, A. Rasheed, J. H. He, A. A. Alsolami, Free vibration of a tapered beam by the Aboodh transformbased variational iteration method, *J. Comput. Appl. Mech,* Vol. 55, pp. 440-450, 2024.

[17] X. Wang, T. A. Elgohary, Z. Zhang, T. H. Tasif, H. Y. Feng, S. N. Atluri, An adaptive local variational iteration method for orbit propagation in astrodynamics problems, *J. Astronaut. Sci,* Vol. 70, 2023.

[18] A. A. Rossikhin, V. I. Mileshin, Application of the harmonic balance method to calculate the first booster stage tonal noise, *Math. Model. Comput. Simul,* Vol. 16, pp. 63-75, 2024.

[19] Q. S. Wang, Z. P. Yan, H. H. Da, An efficient multiple harmonic balance method for computing quasi-periodic responses of nonlinear systems, *J. Sound Vib,* Vol. 554, 2023.

[20] J. Li, Y. F. Xin, T. T. Murmy, Exploring comfort and vibration dampening in fashion design in fabrics with innovative use of nanoparticle additives, *Adv. Nano Res,* Vol. 17, pp. 465-471, 2024.

[21] Y. Zhang, Q. H. Guo, X. H. Wan, L. Y. Zheng, Subwavelength topological edge states in a mechanical analogy of nanoparticle chain, *New J. Phys,* Vol. 27, 2025.

[22] D. Arifin, S. Mcwilliam, Negating self-induced parametric excitation in capacitive ring-based MEMS Coriolis vibrating gyroscopes, *J. Sound Vib,* Vol. 607, 2025.

[23] C. H. He, A variational principle for a fractal nano/microelectromechanical (N/MEMS) system, *Int. J. Numer. Methods Heat Fluid Flow,* Vol. 33, pp. 351-359, 2023.

[24] J. H. He, C. H. He, A. A. Alsolami, Periodic solution of a micro-electromechanical system, *Facta Univ. Ser. Mech. Eng,* Vol. 22, pp. 187-198, 2024.

[25] J. Song, C. Xia, G. S. Shan, Z. Q. Wang, T. Ono, G. G. Cheng, D. F. Wang, Temperature sensing and energy harvesting with a MEMS parametric coupling device under low frequency vibrations, *J. Sound Vib,* Vol. 585, 2024.

[26] Y. O. El-Dib, Stability analysis of a time-delayed Van der Pol-Helmholtz-Duffing oscillator in fractal space with a non-perturbative approach, *Commun. Theor. Phys,* Vol. 76, 2024.

[27] Y. O. El-Dib, N. S. Elgazery, Y. M. Khattab, H. A. Alyousef, An innovative technique to solve a fractal damping Duffing-jerk oscillator, *Commun. Theor. Phys,* Vol. 75, 2023.

[28] G. M. Ismail, G.M. Moatimid, M. I. Yamani, Periodic solutions of strongly nonlinear oscillators using He's frequency formulation, *Eur. J. Pure Appl. Math,* Vol. 17, pp. 2155-2172, 2024.

[29] G. Hashemi, A novel analytical approximation approach for strongly nonlinear oscillation systems based on the energy balance method and He's frequency-amplitude formulation, *Comput. Methods Differ. Equ,* Vol. 11, pp. 464-477, 2023.

[30] J. H. He, The simpler, the better: Analytical methods for nonlinear oscillators and fractional oscillators, *J. Low Freq. Noise Vib. Act. Control,* Vol. 38, pp. 1252-1260, 2019.

[31] M. A. Kawser, M. A. Alim, N. Sharif, Analyzing nonlinear oscillations with He's frequency-amplitude method and numerical comparison in jet engine vibration system, *Heliyon,* Vol. 10, 2024.

[32] K. Tsaltas, An improved one-step amplitude-frequency relation for nonlinear oscillators, *Results Phys,* Vol. 54, 2023.

[33] J. H. He, Frequency-amplitude relationship in nonlinear oscillators with irrational nonlinearities, *Spectr. Mech. Eng. Oper. Res,* Vol. 2, pp. 121-129, 2025.

[34] J. H. He, The simplest approach to nonlinear oscillators, *Results Phys,* Vol. 15, 2019.

[35] Y. O. El-Dib, N. S. Elgazery, A novel pattern in a class of fractal models with the non-perturbative approach, *Chaos Solitons Fractals,* Vol. 164, 2022.

[36] Y. O. El-Dib, N. S. Elgazery, An efficient approach to converting the damping fractal models to the traditional system, *Commun. Nonlinear Sci. Numer. Simul,* Vol. 118, 2023.

[37] Y. O. El-Dib, A dynamic study of a bead sliding on a wire in fractal space with the non-perturbative technique, *Arch. Appl. Mech,* Vol. 94, pp. 571-588, 2024.

[38] G. M. Moatimid, Sliding bead on a smooth vertical rotated parabola: stability configuration, *Kuwait J. Sci,* Vol. 47, pp. 6-21, 2020.